Figure 2 **Anti-moesin autoantibody levels in serum samples from patients with Guillain-Barré syndrome, inflammatory disease controls, and healthy controls**

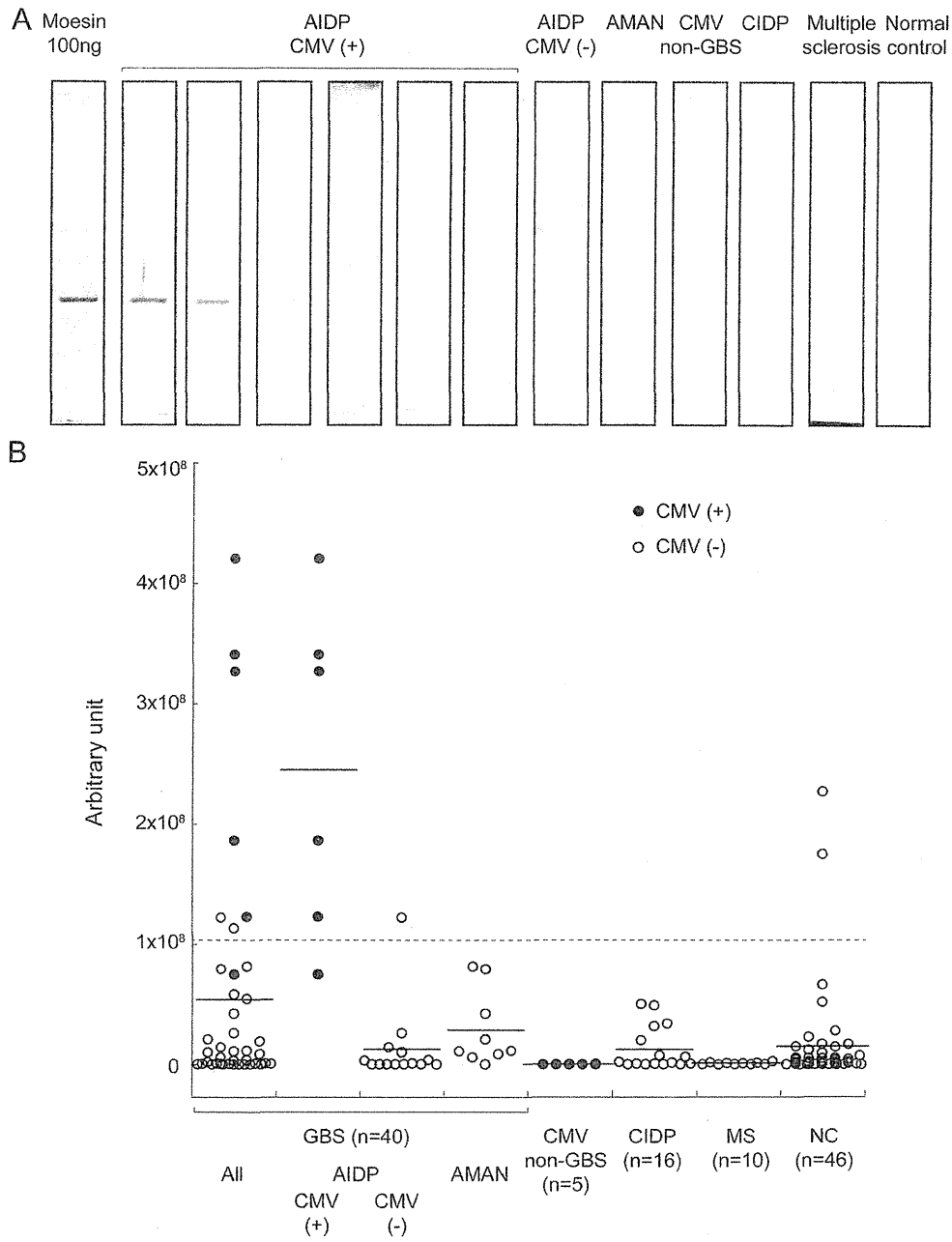

(A) Western blot analysis of serum samples from patients with Guillain-Barré syndrome (GBS) (cytomegalovirus [CMV]-associated acute inflammatory demyelinating polyneuropathy [AIDP], non-CMV-associated AIDP, and acute motor axonal neuropathy [AMAN]), patients with CMV infection without GBS, chronic inflammatory demyelinating polyneuropathy (CIDP), multiple sclerosis (MS), and normal controls (NC) stained with an anti-moesin antibody. "All GBS" included the unclassified patients by electrophysiologic criteria. (B) Densitometry of Western blotting revealed that 83% (5 of 6) individual serum samples from patients with CMV-associated AIDP had anti-moesin autoantibody levels above the cutoff value (dashed line). Solid lines indicate the mean values for each group.

proteins were identified: eukaryotic translation initiation factor 3A (eIF3A), splicing factor 3 subunit 1, septin-11, α-enolase, heterogeneous nuclear ribonucleoproteins A2 and B1, and membrane-organizing extension spike protein (moesin). Of the 6 candidates, only moesin is a plasma membrane protein expressed by Schwann cells (white circle in figure 1; SwissProt accession number: P26038; MOWSE score [top candidate]: 2,136; sequence coverage: 60%).

Of the 40 patients with GBS tested, 7 demonstrated intense immunolabeling of moesin (as indicated by a moesin band density in Western blots

Figure 3 **Subcellular localization of anti-moesin and serum immunofluorescence staining of YST-1 schwannoma cells**

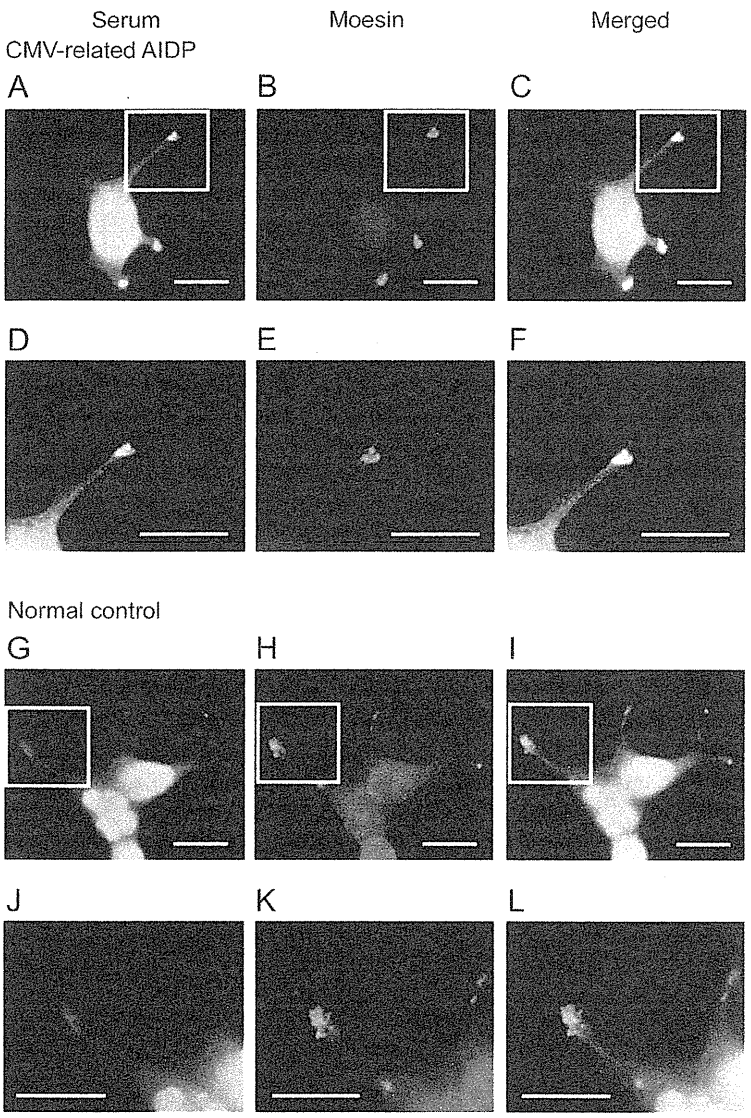

(A–F) Immunostaining pattern of YST-1 cells incubated with serum immunoglobulin G from patients with cytomegalovirus (CMV)-associated acute inflammatory demyelinating polyneuropathy (AIDP) or (G–L) from healthy controls. Panels D–F and J–L are enlarged images of the areas defined by the white boxes in A–C and G–I, respectively. Only serum samples from patients with CMV-associated Guillain-Barré syndrome and moesin monoclonal antibodies labeled the distal tips of YST-1 cells. Bar: 20 μm.

>2 SDs above the mean of healthy controls), including 5 of the 6 patients with CMV-related AIDP (figure 2). Therefore, the majority of patients with CMV-related AIDP (5/6, 83%) had serum anti-moesin antibodies. In contrast, none of the 9 patients with AMAN, one of the 11 patients with unclassified GBS, none of the 5 patients with CMV infection without neuropathy, none of 16 patients with chronic inflammatory demyelinating polyneuropathy, none of 10 patients with MS, and only 2 of the 46 control patients (4%) had serum samples reactive to moesin, suggesting that moesin is a specific autoantigen leading to CMV-related AIDP. In 2 patients with CMV-related AIDP, follow-up studies showed the antibody levels of anti-moesin autoantibodies significantly decreased 3 months and 12 months later, respectively (data not shown).

Immunocytochemistry analyses showed that the distal tips of YST-1 cell processes and leading lamellae were stained strongly by a serum sample from a patient with CMV-related AIDP confirmed to express the anti-moesin autoantibody (figure 3, A–F), whereas no immunofluorescence was detected in healthy controls (figure 3, G–L). Immunohistochemical assessments using mouse sciatic nerves also demonstrated that anti-moesin–positive CMV-related AIDP patient's IgG bound the antigen at the node of Ranvier, which colocalized with moesin (figure e-1 on the *Neurology*® Web site at Neurology.org).

DISCUSSION Whereas it is now established that in AMAN target molecules are glycolipid, immune targets in AIDP would be proteins. Our results show that moesin is a possible target molecule for AIDP after CMV infection. Whereas anti-moesin antibodies were frequently found for patients with CMV-related AIDP, the number of patients was small and only Japanese subjects were studied. These were limitations in this study, and there is a need for a larger study including non-Japanese patients.

Moesin is a member of the ERM family proteins (ezrin, radixin, and moesin). Schwann cells express ERM proteins in microvilli, and local phosphoactivation led to dynamic growth cone-like behavior and node formation at the distal tips in nerve explant cultures,[7] strongly suggesting that moesin has a critical function in myelination. From the immunocytochemistry analysis, serum IgG antibodies of the CMV-related GBS were immunoreactive with moesin at the distal tip of YST-1 (figure 3). The immunostaining pattern was also similar to that previously reported in Schwann cells stained with serum samples from 24% of patients with GBS, although neither the antecedent pathogen nor the antigen at the distal tips was identified.[8]

Anti-moesin autoantibodies were also found in some patients with the paroxysmal nocturnal hemoglobulinuria type of acquired aplastic anemia.[9] However, there is no apparent connection between aplastic anemia and GBS; therefore, it is likely that the anti-moesin antibodies found in patients with these 2 diseases recognize distinct epitopes of the moesin protein.

To establish the molecular mimicry between moesin and CMV proteins, amino acid sequences were analyzed using the BLAST program, which compared 2 protein sequences using a local alignment algorithm. One of the results suggested that 6 consecutive

amino acids (HRGMLR) were matched between moesin and CMV protein "Phosphoprotein 85." This candidate was one of the possible immunologic targets, and further analysis was needed.

Cases of AIDP associated with other antecedent pathogens may arise from other autoantibodies. For example, the nodal/perinodal proteins, such as neurofascin, contactin, and gliomedin, are additional candidate immune targets in patients with GBS. Gliomedin and moesin are colocalized at the node of Ranvier,[10] and therefore both gliomedin and moesin autoantibodies may trigger demyelination at the same or nearby sites, resulting in AIDP. We need to analyze the molecular function of anti-moesin autoantibody to the pathogenesis of AIDP in future studies.

AUTHOR CONTRIBUTIONS

Drs. Sawai, Mori, and Kuwabara designed the study and drafted the manuscript. Drs. Misawa, Beppu, and Sekiguchi contributed the clinical data and serum samples. Drs. Sawai, Satoh, Sogawa, and Mr. Ishige performed proteomic analyses. Ms. Ishibashi, Drs. Noda and Sato measured the anti-moesin autoantibody in the serum samples. Drs. Kazami and Shibuya performed immunohistochemistry. Drs. Matsushita, Kodera, and Nomura supervised the experiments.

ACKNOWLEDGMENT

The authors thank Professor Youji Nagashima for providing the human schwannoma-derived cell line YST-1.

STUDY FUNDING

Supported by Grants-in-Aid for Scientific Research from the Ministry of Education, Culture, Sports, Science and Technology of Japan (S.S., 23790976) and the Research Committee for Neuroimmunological Diseases of the Research on Measures for Intractable Diseases from the Ministry of Health, Welfare and Labour of Japan (S.K.).

DISCLOSURE

S. Sawai, M. Satoh, M. Mori, S. Misawa, K. Sogawa, T. Kazami, M. Ishibashi, M. Beppu, K. Shibuya, T. Ishige, Y. Sekiguchi, K. Noda, K. Sato, K. Matsushita, Y. Kodera, and F. Nomura report no disclosures relevant to the manuscript. S. Kuwabara serves as an editorial board member of the *Journal of the Neurological Sciences*, and as an associate editor of the *Journal of Neurology, Neurosurgery, and Psychiatry*. Go to Neurology.org for full disclosures.

Received September 10, 2013. Accepted in final form February 7, 2014.

REFERENCES

1. Ho TW, Mishu B, Li CY, et al. Guillain-Barré syndrome in northern China: relationship to *Campylobacter jejuni* infection and anti-glycolipid antibodies. Brain 1995;118:597–605.
2. Yuki N, Kuwabara S. Axonal Guillain-Barré syndrome: carbohydrate mimicry and pathophysiology. J Peripher Nerv Syst 2007;12:238–249.
3. Hafer-Macko CE, Sheikh KA, Li CY, et al. Immune attack on the Schwann cell surface in acute inflammatory demyelinating polyneuropathy. Ann Neurol 1996;39:625–635.
4. Asbury AK, Cornblath DR. Assessment of current diagnostic criteria for Guillain-Barré syndrome. Ann Neurol 1990;27(suppl):S21–S24.
5. Kawashima Y, Fukuno T, Satoh M, et al. A simple and highly reproducible method for discovering potential disease markers in low abundance serum proteins. J Electrophor 2009;53:13–18.
6. Satoh M, Haruta-Satoh E, Yamada M, Kado S, Nomura F. Overexpression of hydroxymethylglutaryl CoA synthase 2 and 2,4-dienoyl-CoA reductase in rat pancreas following chronic alcohol consumption. Pancreas 2013;42:475–482.
7. Gatto CL, Walker BJ, Lambert S. Local ERM activation and dynamic growth cones at Schwann cell tips implicated in efficient formation of nodes of Ranvier. J Cell Biol 2003;162:489–498.
8. Kwa MS, van Schaik IN, De Jonge RR, et al. Autoimmunoreactivity to Schwann cells in patients with inflammatory neuropathies. Brain 2003;126:361–375.
9. Takamatsu H, Feng X, Chuhjo T, et al. Specific antibodies to moesin, a membrane-cytoskeleton linker protein, are frequently detected in patients with acquired aplastic anemia. Blood 2007;109:2514–2520.
10. Eshed Y, Feinberg K, Poliak S, et al. Gliomedin mediates Schwann cell-axon interaction and the molecular assembly of the nodes of Ranvier. Neuron 2005;47:215–229.

European Journal of Neurology 2014, 21: 1002–1010 doi:10.1111/ene.12426

Muscle atrophy in chronic inflammatory demyelinating polyneuropathy: a computed tomography assessment

K. Ohyama, H. Koike, M. Katsuno, M. Takahashi, R. Hashimoto, Y. Kawagashira, M. Iijima, H. Adachi, H. Watanabe and G. Sobue

Department of Neurology, Nagoya University Graduate School of Medicine, Nagoya, Japan

Keywords:
chronic inflammatory demyelinating polyneuropathy, computed tomography, muscle atrophy, treatment resistance

Received 25 October 2013
Accepted 24 February 2014

Background and purpose: Muscle atrophy is generally mild in patients with chronic inflammatory demyelinating polyneuropathy (CIDP) compared with the severity and duration of the muscle weakness. Muscle atrophy was evaluated using computed tomography (CT) in patients with CIDP.

Methods: Thirty-one patients with typical CIDP who satisfied the diagnostic criteria for the definite CIDP classification proposed by the European Federation of Neurological Societies and the Peripheral Nerve Society were assessed. The clinicopathological findings in patients with muscle atrophy were also compared with those in patients without atrophy.

Results: Computed tomography evidence was found of marked muscle atrophy with findings suggestive of fatty degeneration in 11 of the 31 patients with CIDP. CT-assessed muscle atrophy was in the lower extremities, particularly in the ankle plantarflexor muscles. Muscle weakness, which reflects the presence of muscle atrophy, tended to be more pronounced in the lower extremities than in the upper extremities in patients with muscle atrophy, whereas the upper and lower limbs tended to be equally affected in patients without muscle atrophy. Nerve conduction examinations revealed significantly greater reductions in compound muscle action potential amplitudes in the tibial nerves of patients with muscle atrophy. Sural nerve biopsy findings were similar in both groups. The functional prognoses after immunomodulatory therapies were significantly poorer amongst patients with muscle atrophy.

Conclusions: Muscle atrophy was present in a subgroup of patients with CIDP, including patients with a typical form of the disease. These patients tended to demonstrate predominant motor impairments of the lower extremities and poorer functional prognoses.

EUROPEAN JOURNAL OF NEUROLOGY
THE OFFICIAL JOURNAL OF THE EUROPEAN FEDERATION OF NEUROLOGICAL SOCIETIES

Introduction

Chronic inflammatory demyelinating polyneuropathy (CIDP) is a form of chronic neuropathy characterized by immune-mediated demyelination [1–5]. The typical form of CIDP is defined as neuropathy with chronically progressive, stepwise or recurrent symmetrical proximal and distal weakness and sensory dysfunction in all extremities, which develops over at least 2 months [6]. For patients with CIDP, immune-modulating therapies such as intravenous immunoglobulin (IVIg), corticosteroids and plasma exchange are the typical first line of treatment. A response to immune-modulating therapies is evident in the majority of patients with CIDP [5–7]; however, certain patients do not sufficiently recover even with combined therapy. Unfavourable prognostic factors can include central nervous system involvement, later onset age, male gender, long disease duration, active demyelination, axonal damage evidenced via nerve biopsy, and the presence of muscle atrophy [4,8–12]. Although it is thought that the degree of muscle atrophy in CIDP is generally mild given the general severity and duration of weakness, some patients demonstrate profound muscle atrophy [8–12]. In particular, muscle atrophy has been described in an atypical form of CIDP called multifocal acquired demyelinating sensory and motor

Correspondence: G. Sobue and H. Koike, Department of Neurology, Nagoya University Graduate School of Medicine, 65 Tsurumai-Cho, Showa-Ku, Nagoya 466-8550, Japan (tel.: +81 52 744 2385; fax: +81 52 744 2384; e-mails: sobueg@med.nagoya-u.ac.jp and koike-haruki@med.nagoya-u.ac.jp).

neuropathy [13]. Conversely, muscle atrophy in patients with typical CIDP has not been well described in the literature.

In this report, muscle atrophy was evaluated using computed tomography (CT) in patients with typical CIDP as defined by the European Federation of Neurological Societies and the Peripheral Nerve Society (EFNS/PNS) criteria. The clinicopathological features of CIDP in patients with muscle atrophy were also characterized.

Patients and methods

Patients

The CT findings of the muscles of 31 patients who met the EFNS/PNS diagnostic criteria for typical CIDP [6] and were referred to the Nagoya University Graduate School of Medicine between January 1999 and February 2013 were retrospectively evaluated. Only patients who met the criteria for 'definite CIDP' were assessed. Because the EFNS/PNS criteria define multifocal acquired demyelinating sensory and motor neuropathy as atypical [6], patients who exhibit lateralized neuropathic involvement were excluded. All patients underwent a clinical and neurological assessment. Patients were assessed for muscle strength using the Medical Research Council scale for the proximal and distal portions of the upper and lower limbs and neck. Sensory deficits were tested in the distal extremities. Functional assessments were performed using the modified Rankin scale (mRS) [14]. Positive response to therapy was defined as improvement in at least one score on the mRS within 3 months of immunomodulatory therapy onset. Patients with CIDP who did not respond to immunomodulatory therapies were followed for at least 2 years to exclude other diseases such as familial amyloid polyneuropathy [15,16]. Patients' sera were tested via an electrophoresis assay to exclude those with monoclonal gammopathy. The Ethics Committee of Nagoya University Graduate School of Medicine approved the study protocol.

Patients received IVIg, corticosteroids, plasmapheresis or a combination of these regimens (Table 2). IVIg was administered at a daily dose of 400 mg/kg for 5 days. In general, corticosteroid therapy was initiated at a daily dose of 1 mg/kg. Intravenous methylprednisolone (1000 mg daily for 3 days) was always followed by oral prednisolone. Between five and seven plasma exchange sessions were performed. A Plasmaflo OP-08W (Asahi Kasei Medical Co., Tokyo, Japan) plasma separator was used for this purpose. Other immunomodulatory therapies such as rituximab, cyclophosphamide and cyclosporine were used to treat four patients.

Muscle CT

Computed tomography scans without intravenous contrast were performed for each patient. The slice thickness was 10 mm, and the radiation doses (expressed in computed tomography dose index volumes) ranged from 7.2 to 16.1 mGy. A CT protocol involving 43 muscles at eight levels was used (Table 1). The muscles were divided into 12 regions, and these regions were assessed in each patient. The windowed CT appearance of each muscle was semiquantitatively graded using the Swash *et al.* [17] scale as follows: grade 0 (normal), a muscle of normal area and attenuation; grade 1 (atrophic), a muscle of reduced area, abnormally clear delineation, and/or containing zones of decreased attenuation; grade 2 (moth-eaten), a muscle containing multiple patchy areas of low attenuation; and grade 3 (washed-out), a muscle of generally low attenuation, with or without focal zones of abnormality, and of reduced area. 'Abnormally clear delineation' for grade 1 was considered to refer to the gaps between muscles. Muscles are closely apposed without gaps in patients without muscle atrophy, such that the boundary between muscles is unclear. Conversely, gaps comprising connective tissues are observed in patients with muscle atrophy. In these cases, the delineation of each muscle becomes abnormally clear. Because the assessment of muscle atrophy was based on visual interpretation, two independent observers verified the concordance between different evaluators' assessments.

Table 1 Muscles evaluated via CT

Level	Muscles
Third cervical vertebra	Rotators, multifidus muscles, semispinalis capitis, semispinalis cervicis, splenius capitis
Second thoracic vertebra	Subscapularis, infraspinatus, deltoid
Middle of the arm	Biceps, brachialis, triceps
Greatest diameter of the forearm	Brachioradialis, extensor carpi radialis, extensor digitorum, extensor carpi ulnaris, flexor carpi radialis, flexor digitorum superficialis, flexor carpi ulnaris, flexor digitorum profundus
Iliac crest	Psoas major, transversospinal muscles, erector spinae
Pubic symphysis	Iliopsoas, gluteus medius, gluteus minimus, gluteus major
Middle of the thigh	Rectus femoris, vastus medialis, vastus intermedius, vastus lateralis, sartorius, adductor magnus, gracilis, semimembranosus, semitendinosus, biceps femoris
Greatest diameter of the calf	Extensor hallucis longus, extensor digitorum longus, tibialis anterior, gastrocnemius, soleus, peroneus brevis, flexor hallucis longus

Evaluators' assessments were mostly concordant; differences between them were <5%. CT images were reviewed by two of the authors blinded to patient clinical information. These observers later compared the CT findings and agreed on the interpretation of these images. The CT cross-sectional areas of the extremities were also assessed using RapideyeCore (Toshiba Medical Systems Corporation, Otawara, Japan).

In this study, patients were considered to exhibit 'marked muscle atrophy' when they demonstrated muscle atrophy of grades 2 or 3 in at least two muscles in which fatty muscle degeneration was suggested.

Electrophysiological examination

Each patient completed a nerve conduction study. Motor and sensory nerve conduction was measured in the median, ulnar, tibial, peroneal and sural nerves using a standard method with surface electrodes for stimulation and recording [18,19]. The compound muscle action potential (CMAP) and sensory nerve action potential amplitudes were measured from baseline to the first negative peak. A conduction block was defined using the EFNS/PNS electrodiagnostic criteria [6]. The distal CMAP duration was measured from the onset of the action potential to the first crossing of the baseline. The normal control values were based on our previously published reports [18,19].

Needle electromyography (EMG) was performed with concentric needles in the deltoid, biceps brachii, first dorsal interosseous, thenar, lumbar paraspinal, quadriceps and tibialis anterior muscles. Spontaneous denervation activity was defined as fibrillation potentials, positive sharp waves, or both.

Pathological examination of sural nerve biopsy specimens

Histopathological examinations of sural nerve specimens were performed in 22 of the 31 patients. The specimens were fixed in 2.5% glutaraldehyde in a 0.125 M cacodylate buffer (pH 7.4) and embedded in epoxy resin [20,21]. The density of the myelinated fibres was assessed in toluidine-blue-stained semi-thin sections using a computer-assisted image analyser (Luzex FS; Nikon, Tokyo, Japan) as previously described [21,22]. A fraction of the glutaraldehyde-fixed sample was processed for a teased-fibre study. The normal control values were based on a previously published report [18].

Data analyses

Quantitative data are presented as mean ± SD. Student's t test was used to analyse the parametric variables, and the Mann–Whitney U test was used for the non-parametric variables. The chi-squared test and Fisher's exact test were used for categorical variables. To determine the relationships between the cross-sectional area, electrophysiological indices and muscle atrophy, Pearson's or Spearman's correlation analyses were conducted when appropriate. For these comparisons, $P < 0.05$ was considered significant.

Results

Of the 31 CT scans, 11 demonstrated muscle atrophy of grade 2 or 3 in at least two muscles. These patients were considered as exhibiting 'marked muscle atrophy' with fatty degeneration. Four of the remaining 20 patients demonstrated grade 1 muscle atrophy in the trunk and leg regions; no muscle atrophy was detected in the remaining 16 patients. Leg muscles were atrophied at higher frequencies and with greater severity than arm muscles; the most frequently atrophied muscles were the ankle plantarflexors (Fig. 1). Thus, patients with muscle atrophy tended to exhibit conspicuous muscle atrophy in the lower legs, rather than diffuse atrophy (Data S1). Although the location of the muscle atrophy revealed by the CT examination corresponded to that found via visual inspection to a certain extent, some patients demonstrated extensive fatty degeneration without a significantly reduced cross-sectional area. Therefore, no correlation was found between the cross-sectional area and the Swash criteria (Data S2). Typical CT examples of muscle atrophy in the lower extremities are shown in Fig. 2.

The clinical profiles of the patients with CIDP at the time of the CT examination are shown in Table 2. No differences were observed between the patients with marked muscle atrophy and those without in terms of gender, disease duration or treatment response. The prevalence of muscle atrophy was higher amongst patients with longer disease durations prior to their CT scan or treatment initiation. However, patients with marked muscle atrophy did not significantly differ from those without marked muscle atrophy with regard to disease duration (Table 2), most probably because some patients experienced muscle atrophy in the early phase of neuropathy (Fig. 3). The severity of muscle weakness and sensory disturbance was similar between the two groups; however, significantly more prominent muscle weakness was observed in the distal portions of their lower extremities in patients with marked muscle atrophy than in those without marked muscle atrophy ($P < 0.01$). Muscle weakness and atrophy tended to predominate in the lower extremities of patients with marked muscle atrophy, whereas the upper and lower

limbs tended to be equally affected amongst patients without marked atrophy. Patient functional status (as determined by the mRS) was similar prior to treatment between the two groups. After treatment, however, the mRS was significantly improved amongst patients without marked muscle atrophy ($P < 0.05$).

The cerebrospinal fluid examination revealed elevated protein levels in 10 patients (91%) with marked muscle atrophy and 18 patients (86%) without marked muscle atrophy. The difference in protein concentration was not significant between the two groups. Magnetic resonance imaging (MRI) revealed a gadolinium enhancement of the cauda equina in six patients (55%) with marked muscle atrophy and 12 patients (60%) without marked atrophy; however, these differences were not significant.

The results of the nerve conduction studies are summarized in Table 3. The motor nerve conduction velocities, sensory nerve conduction velocities and distal motor latencies were similar between patient groups. However, the CMAP of the tibial nerves was significantly reduced amongst patients with marked muscle atrophy compared with those without marked atrophy ($P < 0.05$). Conversely, the CMAP duration in the tibial nerves was significantly longer amongst patients without marked atrophy ($P < 0.05$). A significant correlation was not found between the CMAP and the Swash muscle atrophy grade of the corresponding innervated muscles, even in the calf ($P = 0.20$ and $P = 0.33$ for the tibial and peroneal nerves, respectively; Spearman's rank correlation coefficient) where muscle atrophy was the most salient. The EMG findings did not differ significantly between the two groups (Data S3).

Nerve biopsies were performed for nine patients with marked muscle atrophy and 13 patients without marked muscle atrophy. Significant differences were not observed between the two groups (Data S3).

Discussion

Marked muscle atrophy with findings suggestive of fatty degeneration was detected via CT in one-third of our patients with CIDP, which matches previously reported rates [9–11]. However, sample bias must be considered because refractory cases tend to be referred to our institution. Nevertheless, muscle atrophy was observed even in patients with typical CIDP. Muscle atrophy tended to predominate in the lower legs. Muscle atrophy was also detected in the early phase of the disease for some patients.

Computed tomography was used to assess muscle atrophy for two reasons. First, CT is able to obtain whole-body images quickly. One of the purposes of this study was to characterize the frequency and distribution (e.g. the upper limbs, lower limbs or trunk) of muscle atrophy in patients with CIDP. Therefore, it is believed that CT is more appropriate than MRI. Secondly, CT is more cost effective and widely available than MRI. Although MRI can provide additional information to detect minute changes and qualitative abnormalities such as inflammation [23,24], the cost and availability of CT are important. Certain patients exhibited extensive fatty degeneration without significantly reduced cross-sectional area; thus, a strong correlation between the cross-sectional area of the extremities and the Swash muscle atrophy grade [17] was not found. Therefore,

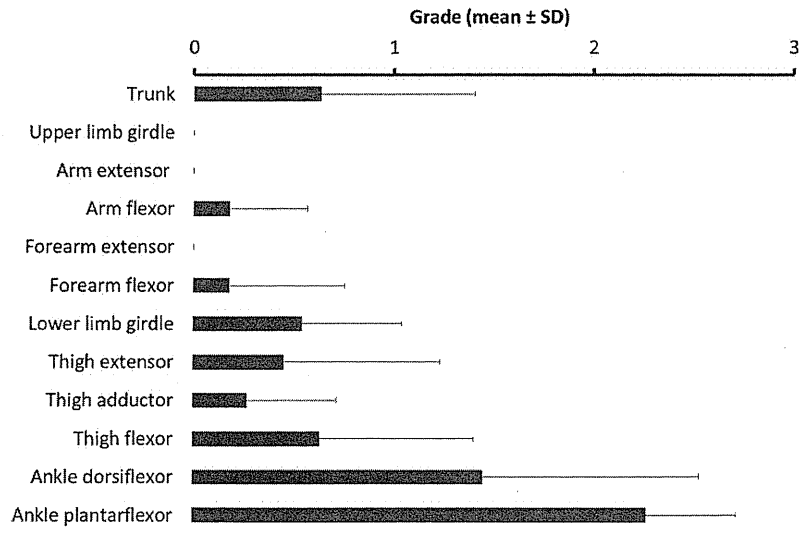

Figure 1 The distribution of muscle atrophy amongst patients with CIDP with marked muscle atrophy ($n = 11$). The atrophy of each muscle was graded using the Swash *et al.* criteria [17] via CT images. The highest grade for the atrophied muscles in each region was analysed. Muscle atrophy was most prominent in the legs and predominated in the ankle plantarflexor muscles.

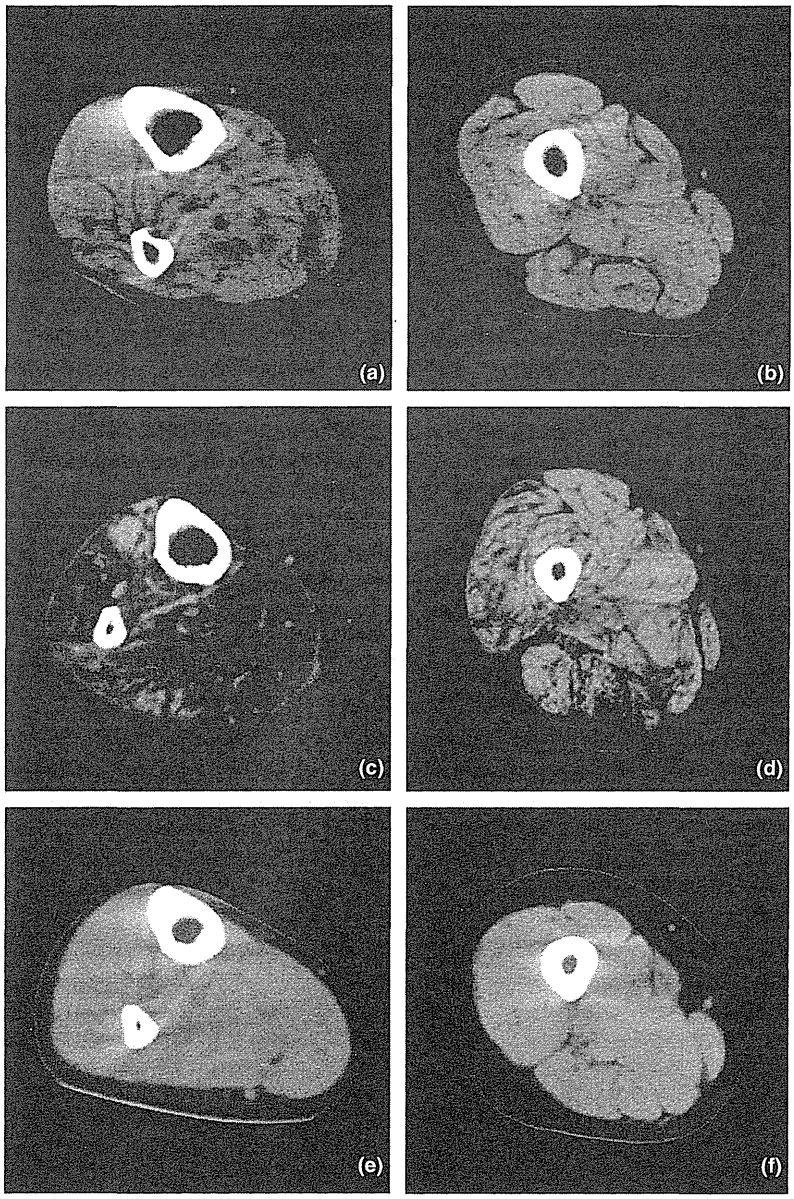

Figure 2 Muscle CT of the lower extremities. Images (a) and (b) were obtained from one patient with marked muscle atrophy 3 months after the onset of CIDP. The image of the lower leg (a) demonstrates multiple patchy areas of low attenuation in the ankle plantarflexor muscles (grade 2). Conversely, the image of the thigh (b) shows abnormally clear delineation (grade 1). Images (c) and (d) were obtained from a second patient with marked muscle atrophy 87 months after the onset of CIDP. The image of the lower leg (c) demonstrates diffuse low attenuation in the ankle dorsiflexor and plantarflexor muscles (grade 3). The image of the thigh (d) shows multiple patchy areas of low attenuation (grade 2). Images (e) and (f) were obtained from a patient who did not have muscle atrophy. The muscle CT of this patient 8 months after onset did not reveal muscle atrophy (grade 0); however, this patient reported severe weakness of the ankle dorsiflexor and plantarflexor muscles.

it is proposed that the Swash scale is more appropriate than visual inspection or cross-sectional area when assessing muscle atrophy in patients with CIDP.

The mechanisms of muscle atrophy in patients with CIDP are not fully understood. Muscle atrophy caused by axonal damage due to the disruption of axon–Schwann cell interactions has been described in other demyelinating neuropathies [25–28]. For example, distally accentuated muscle wasting is correlated with axonal degeneration resulting in decreased CMAP amplitude amongst patients with Charcot–Marie–Tooth disease type 1A [25–27]. PMP22 abnormalities result in impaired axonal cytoskeletal organization, including an increase in neurofilament density, and lead to axonal atrophy and degeneration [29–31]. In addition, IgM deposits have been observed in paranodal regions in patients with IgM-monoclonal gammopathy of undetermined significance with anti-myelin-associated glycoprotein (anti-MAG) neuropathy; demyelination also occurs in paranodal regions and might cause axonal damage [28]. The absence of MAG or the presence of anti-MAG antibodies results in axonal atrophy and the degeneration of myelinated fibres [32,33]. The pathological hallmarks of CIDP are segmented demyelination and

Table 2 Patient clinical profiles

	Muscle atrophy + (grade 2 or 3)	Muscle atrophy − (grade 0 or 1)	*P*
Number of patients	11	20	
Gender (Male : Female)	7 : 4	14 : 6	NS
Age of onset[a]	41 ± 21	43 ± 17	NS
Disease duration (months)			
Onset to initial treatment[a]	22 ± 29	10 ± 13	NS
Onset to CT[a]	74 ± 65	34 ± 40	NS
Therapy in our hospital			
IVIg[b]	9 (82%)	19 (95%)	NS
PSL[b]	5 (45%)	12 (60%)	NS
PE[b]	1 (9%)	1 (5%)	NS
Response to therapy[b]	6 (55%)	15 (75%)	NS
Weakness (MRC scale)			
Neck[a]	5	4.9 ± 0.5	NS
Upper limb proximal[a]	4.2 ± 0.9	4.0 ± 1.1	NS
Upper limb distal[a]	3.4 ± 0.9	3.5 ± 1.1	NS
Lower limb proximal[a]	3.8 ± 0.9	3.8 ± 1.1	NS
Lower limb distal[a]	2.5 ± 0.5	3.6 ± 1.0	<0.01
Sensory disturbance			
Spontaneous[b]	8 (73%)	14 (70%)	NS
Pain[b]	5 (45%)	10 (50%)	NS
Touch[b]	4 (36%)	8 (40%)	NS
Vibration[b]	7 (64%)	15 (75%)	NS
Joint position[b]	2 (18%)	7 (35%)	NS
mRS before treatment[a,c]	2.7 ± 0.6	2.7 ± 0.9	NS
mRS after treatment[a,c]	2.2 ± 0.4	1.7 ± 0.7	<0.05
CSF protein (mg/dl)[a]	103 ± 87	165 ± 139	NS
Gd enhancement of the cauda equina[b]	6 (55%)	12 (60%)	NS

IVIg, intravenous immunoglobulin; PSL, prednisolone; PE, plasma exchange; MRC, Medical Research Council; mRS, modified Rankin scale; CSF, cerebrospinal fluid; Gd, gadolinium; NS, not significant. [a]Data shown are mean ± SD; [b]data shown are the number and percentage of positive patients; [c]modified Rankin scale (mRS) [14] with the following coding system: 0, asymptomatic; 1, non-disabling symptoms that do not interfere with lifestyle; 2, minor disability from symptoms leading to certain lifestyle restrictions, but no interference with capacity for self-care; 3, moderate disability from symptoms that significantly interfere with lifestyle or prevent an independent existence; 4, moderately severe disability from symptoms clearly precluding independent living but not requiring 24 h attention from a caregiver; 5, severe disability and total dependence, requiring constant attention.

re-myelination of the peripheral nerves with inflammatory cellular infiltrations. However, axonal degeneration is also found in patients with CIDP [1,3–5,9]. A recent electrophysiological study suggested that \immunomodulatory therapies improve axonal function in patients with CIDP [34].

In our study, muscle atrophy was salient in the lower extremities; therefore, the presence of muscle weakness was more evident in the lower extremities than in upper

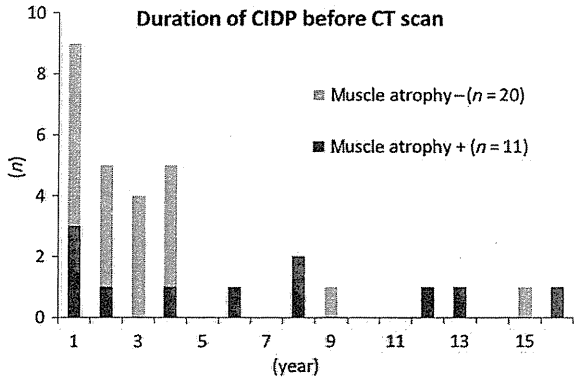

Figure 3 The association of muscle atrophy and disease duration prior to CT. Certain patients with CIDP experience muscle atrophy during the early phase of the disease.

extremities in patients with marked muscle atrophy, whilst the upper and lower limbs tended to be equally affected in patients without muscle atrophy. Electrophysiological findings also indicated more prominent abnormalities that were suggestive of axonal dysfunction (i.e. CMAP amplitude) in the lower extremities of patients with marked muscle atrophy. Conversely, abnormalities suggestive of demyelination (i.e. CMAP duration) were more prominent amongst patients without muscle atrophy. These findings suggest that factors related to the maintenance of peripheral nerve axons (rather than those related to demyelination) are affected in patients with muscle atrophy. These abnormalities might affect axons and lead to degeneration in distal axonal regions. However, axonal degeneration of the sural nerve was not evident in either group of the present study. Because weakness was more predominant than sensory disturbance in most patients, the scarcity of sensory involvement might have influenced the axonal degeneration in the sural nerve, which was lower than expected. Previous studies have reported that muscle atrophy, CMAP amplitude reduction and polymorphisms of the transient axonal glycoprotein-1 (TAG-1) gene are related to IVIg responsiveness in patients with CIDP [12]. TAG-1 probably maintains axonal function in the peripheral nervous system [35]. Therefore TAG-1 polymorphisms might be associated with axonal damage and muscle atrophy [35].

In conclusion, muscle atrophy was present in a subgroup of patients with CIDP, even those with a typical form of the disease. These patients tended to demonstrate a predominant involvement of the lower extremities and poorer functional prognoses. Additional studies are needed to describe the mechanisms that underlie muscle atrophy in this form of CIDP.

Table 3 Electrophysiological abnormalities

	Muscle atrophy + (grade 2 or 3)	Muscle atrophy − (grade 0 or 1)	*P*	Normal control
Nerve conduction studies				
Number of patients	11	20		
Motor				
Median				
MCV (m/s)[a]	39.7 ± 13.7	37.0 ± 14.5	NS	57.6 ± 3.8
DL (ms)[a]	5.3 ± 2.0	8.1 ± 5.0	NS	3.4 ± 0.4
Distal CMAP duration (ms)[a]	6.1 ± 1.3	6.3 ± 1.7	NS	4.7 ± 0.9
CMAP (mV)[a]	3.1 ± 2.5	4.3 ± 3.3	NS	8.2 ± 2.9
CB[b]	1 (9%)	3 (15%)	NS	
FL (ms)[a]	48.0 ± 16.5	36.1 ± 9.3	NS	22.3 ± 1.9
FO (%)[a]	23.9 ± 32.3	25.6 ± 33.1	NS	67.6 ± 20.3
Ulnar				
MCV (m/s)	42.1 ± 14.6	35.1 ± 16.3	NS	58.0 ± 4.6
DL (ms)	4.3 ± 2.5	5.3 ± 2.4	NS	2.6 ± 0.3
Distal CMAP duration (ms)	5.8 ± 1.2	7.1 ± 2.3	NS	5.1 ± 0.7
CMAP (mV)	4.8 ± 3.4	4.5 ± 2.9	NS	7.4 ± 1.8
CB	1 (9%)	2 (10%)	NS	
Tibial				
MCV (m/s)	34.7 ± 9.5	35.5 ± 8.7	NS	46.0 ± 3.8
DL (ms)	6.8 ± 2.5	7.9 ± 3.1	NS	4.0 ± 0.6
Distal CMAP duration (ms)	5.1 ± 3.1	7.2 ± 2.3	<0.05	5.0 ± 0.7
CMAP (mV)	0.6 ± 1.1	3.3 ± 4.4	<0.05	11.8 ± 3.5
CB	0 (0%)	1 (5%)	NS	
FL (ms)	60.6 ± 17.0	59.5 ± 17.2	NS	41.4 ± 3.0
FO (%)	21.2 ± 36.8	38.8 ± 48.8	NS	96.3 ± 12.5
Peroneal				
MCV (m/s)	34.3 ± 5.9	33.1 ± 13.3	NS	47.4 ± 4.5
DL (ms)	5.5 ± 0.4	11.0 ± 8.3	NS	4.6 ± 1.1
Distal CMAP duration (ms)	5.2 ± 1.8	7.6 ± 2.3	NS	4.9 ± 0.9
CMAP (mV)	0.3 ± 0.3	0.9 ± 1.3	NS	3.4 ± 2.0
CB	1 (9%)	1 (5%)	NS	
Sensory				
Median				
SCV (m/s)[a]	43.6 ± 18.0	41.3 ± 11.4	NS	56.3 ± 5.3
SNAP (μV)[a]	8.5 ± 13.6	7.4 ± 9.5	NS	28.0 ± 11.5
Ulnar				
SCV (m/s)	41.5 ± 13.6	39.0 ± 9.4	NS	54.5 ± 5.5
SNAP (μV)	8.4 ± 12.6	5.9 ± 9.3	NS	23.8 ± 10.3
Sural				
SCV (m/s)	41.1 ± 8.1	46.8 ± 8.4	NS	49.2 ± 4.8
SNAP (μV)	8.4 ± 12.4	13.1 ± 15.6	NS	16.8 ± 7.8

MCV, motor nerve conduction velocity; DL, distal latency; CMAP, compound muscle action potential; CB, conduction block; FL, F-wave latency; FO, F-wave occurrence; SCV, sensory nerve conduction velocity; SNAP, sensory nerve action potential; NS, not significant.
Control values are based on a previously published report [18,19]. [a]Data are shown as the mean ± SD; [b]data are shown as the number and percentage of positive patients.

Acknowledgements

Grants from the Ministry of Health, Labor, and Welfare and the Ministry of Education, Culture, Sports, Science, and Technology of Japan supported this research.

Disclosure of conflict of interest

The authors declare no financial or other conflicts of interest.

Supporting Information

Additional Supporting Information may be found in the online version of this article:

Data S1. The distribution of muscle atrophy.
Data S2. Correlation of cross-sectional area and muscle atrophy grade.
Data S3. Electrophysiological and pathological abnormalities.

References

1. Dyck PJ, Lais AC, Ohta M, Bastron JA, Okazaki H, Groover RV. Chronic inflammatory polyradiculoneuropathy. *Mayo Clin Proc* 1975; **50:** 621–637.
2. McCombe PA, Pollard JD, McLeod JG. Chronic inflammatory demyelinating polyradiculoneuropathy. A clinical and electrophysiological study of 92 cases. *Brain* 1987; **110:** 1617–1630.
3. Barohn RJ, Kissel JT, Warmolts JR, Mendell JR. Chronic inflammatory demyelinating polyradiculoneuropathy. Clinical characteristics, course, and recommendations for diagnostic criteria. *Arch Neurol* 1989; **46:** 878–884.
4. Bouchard C, Lacroix C, Planté V, *et al.* Clinicopathologic findings and prognosis of chronic inflammatory demyelinating polyneuropathy. *Neurology* 1999; **52:** 498–503.
5. Vallat JM, Sommer C, Magy L. Chronic inflammatory demyelinating polyradiculoneuropathy: diagnostic and therapeutic challenges for a treatable condition. *Lancet Neurol* 2010; **9:** 402–412.
6. Van den Bergh PY, Hadden RD, Bouche P, *et al.* European Federation of Neurological Societies; Peripheral Nerve Society. European Federation of Neurological Societies/Peripheral Nerve Society guideline on management of chronic inflammatory demyelinating polyradiculoneuropathy: report of a joint task force of the European Federation of Neurological Societies and the Peripheral Nerve Society – first revision. *Eur J Neurol* 2010; **17:** 356–363.
7. Viala K, Maisonobe T, Stojkovic T, *et al.* A current view of the diagnosis, clinical variants, response to treatment and prognosis of chronic inflammatory demyelinating polyradiculoneuropathy. *J Peripher Nerv Syst* 2010; **15:** 50–56.
8. Wertman E, Argov Z, Abrmasky O. Chronic inflammatory demyelinating polyradiculoneuropathy: features and prognostic factors with corticosteroid therapy. *Eur Neurol* 1988; **28:** 199–204.
9. Hattori N, Misu K, Koike H, *et al.* Age of onset influences clinical features of chronic inflammatory demyelinating polyneuropathy. *J Neurol Sci* 2001; **184:** 57–63.
10. Iijima M, Yamamoto M, Hirayama M, *et al.* Clinical and electrophysiologic correlates of IVIg responsiveness in CIDP. *Neurology* 2005; **64:** 1471–1475.
11. Kuwabara S, Misawa S, Mori M, Tamura N, Kubota M, Hattori T. Long term prognosis of chronic inflammatory demyelinating polyneuropathy: a five year follow up of 38 cases. *J Neurol Neurosurg Psychiatry* 2006; **77:** 66–70.
12. Iijima M, Tomita M, Morozumi S, *et al.* Single nucleotide polymorphism of TAG-1 influences IVIg responsiveness of Japanese patients with CIDP. *Neurology* 2009; **73:** 1348–1352.
13. Viala K, Renié L, Maisonobe T, *et al.* Follow-up study and response to treatment in 23 patients with Lewis–Sumner syndrome. *Brain* 2004; **127:** 2010–2017.
14. van Swieten JC, Koudstaal PJ, Visser MC, Schouten HJ, van Gijn J. Interobserver agreement for the assessment of handicap in stroke patients. *Stroke* 1988; **19:** 604–607.
15. Koike H, Hashimoto R, Tomita M, *et al.* Diagnosis of sporadic transthyretin Val30Met familial amyloid polyneuropathy: a practical analysis. *Amyloid* 2011; **18:** 53–62.
16. Mathis S, Magy L, Diallo L, Boukhris S, Vallat JM. Amyloid neuropathy mimicking chronic inflammatory demyelinating polyneuropathy. *Muscle Nerve* 2012; **45:** 26–31.
17. Swash M, Brown MM, Thakkar C. CT muscle imaging and the clinical assessment of neuromuscular disease. *Muscle Nerve* 1995; **18:** 708–714.
18. Koike H, Hirayama M, Yamamoto M, *et al.* Age associated axonal features in HNPP with 17p11.2 deletion in Japan. *J Neurol Neurosurg Psychiatry* 2005; **76:** 1109–1114.
19. Suzuki K, Katsuno M, Banno H, *et al.* CAG repeat size correlates to electrophysiological motor and sensory phenotypes in SBMA. *Brain* 2008; **131:** 229–239.
20. Sobue G, Hashizume Y, Mukai E, Hirayama M, Mitsuma T, Takahashi A. X-linked recessive bulbospinal neuronopathy. A clinicopathological study. *Brain* 1989; **112:** 209–232.
21. Koike H, Iijima M, Sugiura M, *et al.* Alcoholic neuropathy is clinicopathologically distinct from thiamine-deficiency neuropathy. *Ann Neurol* 2003; **54:** 19–29.
22. Koike H, Iijima M, Mori K, *et al.* Neuropathic pain correlates with myelinated fibre loss and cytokine profile in POEMS syndrome. *J Neurol Neurosurg Psychiatry* 2008; **79:** 1171–1179.
23. Tomasová Studynková J, Charvát F, Jarosová K, Vencovsky J. The role of MRI in the assessment of polymyositis and dermatomyositis. *Rheumatology (Oxford)* 2007; **46:** 1174–1179.
24. Theodorou DJ, Theodorou SJ, Kakitsubata Y. Skeletal muscle disease: patterns of MRI appearances. *Br J Radiol* 2012; **85:** e1298–e1308.
25. Thomas PK, Marques W Jr, Davis MB, *et al.* The phenotypic manifestations of chromosome 17p11.2 duplication. *Brain* 1997; **120:** 465–478.
26. Krajewski KM, Lewis RA, Fuerst DR, *et al.* Neurological dysfunction and axonal degeneration in Charcot–Marie–Tooth disease type 1A. *Brain* 2000; **123:** 1516–1527.
27. Hattori N, Yamamoto M, Yoshihara T, *et al.* Study Group for Hereditary Neuropathy in Japan. Demyelinating and axonal features of Charcot–Marie–Tooth disease with mutations of myelin-related proteins (PMP22, MPZ and Cx32): a clinicopathological study of 205 Japanese patients. *Brain* 2003; **126:** 134–151.
28. Kawagashira Y, Koike H, Tomita M, *et al.* Morphological progression of myelin abnormalities in IgM-monoclonal gammopathy of undetermined significance anti-myelin-associated glycoprotein neuropathy. *J Neuropathol Exp Neurol* 2010; **69:** 1143–1157.
29. de Waegh SM, Lee VM, Brady ST. Local modulation of neurofilament phosphorylation, axonal caliber, and slow axonal transport by myelinating Schwann cells. *Cell* 1992; **68:** 451–463.
30. Sahenk Z, Chen L, Mendell JR. Effects of PMP22 duplication and deletions on the axonal cytoskeleton. *Ann Neurol* 1999; **45:** 16–24.
31. Nobbio L, Gherardi G, Vigo T, *et al.* Axonal damage and demyelination in long-term dorsal root ganglia cultures from a rat model of Charcot–Marie–Tooth type 1A disease. *Eur J Neurosci* 2006; **23:** 1445–1452.

32. Yin X, Crawford TO, Griffin JW, *et al.* Myelin-associated glycoprotein is a myelin signal that modulates the caliber of myelinated axons. *J Neurosci* 1998; **18:** 1953–1962.
33. Lunn MP, Crawford TO, Hughes RA, Griffin JW, Sheikh KA. Anti-myelin-associated glycoprotein antibodies alter neurofilament spacing. *Brain* 2002; **125:** 904–911.
34. Lin CS, Krishnan AV, Park SB, Kiernan MC. Modulatory effects on axonal function after intravenous immunoglobulin therapy in chronic inflammatory demyelinating polyneuropathy. *Arch Neurol* 2011; **68:** 862–869.
35. Iijima M, Koike H, Katsuno M, Sobue G. Polymorphism of transient axonal glycoprotein-1 in chronic inflammatory demyelinating polyneuropathy. *J Peripher Nerv Syst* 2011; **16:** 52–55.

Anti-neutral glycolipid antibodies in encephalomyeloradiculoneuropathy

Sayuri Shima, MD
Naoki Kawamura, MD
Tomomasa Ishikawa, MD
Hiromi Masuda, PhD
Chihiro Iwahara, PhD
Yoshiki Niimi, MD
Akihiro Ueda, MD, PhD
Kazuhiza Iwabuchi, PhD
Tatsuro Mutoh, MD, PhD

Correspondence to Dr. Mutoh: tmutoh@fujita-hu.ac.jp

ABSTRACT

Objective: The aim of this study was to review 4 patients with encephalomyeloradiculoneuropathy (EMRN) and assess for autoantibodies against neutral glycolipids.

Methods: We studied the progression of clinical, radiologic, neurophysiologic, and CSF findings, as well as anti-neutral glycolipid antibodies in sera.

Results: All patients developed acute or subacute motor weakness and impaired consciousness. Their CSF showed pleocytosis and high immunoglobulin G concentrations. MRI revealed lesions in the brain and spinal cord. Neurophysiologic examinations indicated dysfunction of the spinal cord, nerve roots, and peripheral nerves. Steroid pulsed immunotherapy and/or high dose of IV immunoglobulin replacement therapy resulted in clear and often dramatic clinical improvements. Reactivity to anti-neutral glycolipid antibodies was positive in all patients with acute EMRN but not in the recovery phase. Forty-seven age-matched patients with other neurologic disorders and 28 age-matched healthy volunteers tested negative for reactivity to anti-neutral glycolipid antibodies.

Conclusion: The resolution of radiologic and neurologic abnormalities and altered autoantibody titers against neutral glycolipids after immunotherapy suggest that EMRN is caused by an immune-mediated mechanism. These autoantibodies may be useful biomarkers for EMRN.
Neurology® 2014;82:114–118

GLOSSARY

EMRN = encephalomyeloradiculoneuropathy; **GalCer** = galactosylceramide; **GSL** = glycosphingolipid; **LacCer** = lactosylceramide; **PNS** = peripheral nervous system.

Cellular or humoral immunologic dysfunction is one cause of demyelinating disorders of the CNS and peripheral nervous system (PNS). There is evidence that sera of patients with CNS diseases, such as multiple sclerosis[1] and acute disseminated encephalomyelitis,[2] or PNS diseases have in vivo and in vitro reactivity against various components of the CNS and PNS.[1]

The literature contains descriptions of patients with encephalomyeloradiculoneuropathy (EMRN).[3,4] Some authors have portrayed EMRN as acute disseminated encephalomyelitis with Guillain-Barré syndrome or as combined central and peripheral inflammatory demyelination.[5,6]

We previously reported antibodies against glucosylceramide in the sera of patients with relapsing polychondritis with limbic encephalitis.[7] Herein, we describe 4 patients with EMRN whose sera tested positive for anti-neutral glycosphingolipid (GSL) antibodies.

METHODS **Patient 1.** A 50-year-old woman was hospitalized for viral meningitis after a flu-like illness, and 1 month later was transferred to our hospital because of worsening symptomatology. Examination revealed decreased level of consciousness, tetraplegia, and hyperreflexia without pathologic reflexes, left-sided Horner syndrome, facial hyperesthesia, and urinary incontinence (table). Serum autoantibodies, anti–aquaporin-4 antibody tests, antiviral antibody titers, and real-time PCR assays were negative. CSF findings were abnormal (table). Brain fluid-attenuated inversion recovery–weighted and T2-weighted MRI showed lesions with high signal intensity (figure 1A), and brain SPECT showed increased uptake in the same regions (figure 1C). Cervical MRI revealed an edematous spinal cord and long cord lesions with high signal intensity (figure 1B). Nerve conduction studies showed decreased amplitude of compound muscle action potentials and sensory nerve action potentials with absence of F waves in several nerves. Auditory brainstem response and somatosensory evoked potential were also abnormal.

Supplemental data at www.neurology.org

From the Department of Neurology (S.S., N.K., T.I., Y.N., A.U., T.M.), Fujita Health University School of Medicine, Aichi; and Institute for Environmental and Gender Specific Medicine (H.M., C.I., K.I.), Juntendo University Graduate School of Medicine, Chiba, Japan.
Go to Neurology.org for full disclosures. Funding information and disclosures deemed relevant by the authors, if any, are provided at the end of the article.

Table Clinical characteristics of 4 patients with EMRN

	Patient 1	Patient 2	Patient 3	Patient 4
Age, y/sex	50/F	49/M	26/M	76/F
Antecedent event	Viral meningitis	Flu	Flu	—
Weakness, MRC scale	2-3	3-4	2-3	4-5
GCS score on admission	11 (2-4-5)	11 (2-4-5)	11 (2-4-5)	14 (3-5-6)
Autonomic dysfunction	+ (inconti., Horner syndrome)	+ (ileus, inconti., unstable BP)	+ (inconti.)	+ (unstable BP, constipation)
Cell no. in CSF /mm^3	109	116	70	43
Protein level/IgG in CSF, mg/dL	81/10	192/43	173/19	65/12
Real-time PCR in CSF (EBV, HSV, CMV, HHV6, 7)	–	–	–	–
Neurophysiologic study	Mainly A	A + D	Mainly A	A + D
CMAP and SNAP↓	+	+	+	+
NCV↓	–	+	–	+
F-wave frequency, %	0	0	0	0
ABR, SEP abnormality	+	+	+	+
Antibody titer in sera LacCer/GalCer/GlcCer	2+/–/–[a]	3+/1+/–[a]	2+/±/–[a]	2+/–/–[a]

Abbreviations: A = axonal; ABR = auditory brainstem response; BP = blood pressure; CMAP = compound muscle action potential; CMV = cytomegalovirus; D = demyelination; EBV = Epstein-Barr virus; EMRN = encephalomyeloradiculoneuropathy; GalCer = anti-galactosylceramide antibody in serum; GCS = Glasgow Coma Scale; GlcCer = anti-glucosylceramide antibody in serum; HHV6 = human herpesvirus 6; HHV7 = human herpesvirus 7; HSV = herpes simplex virus; IgG = immunoglobulin G; inconti. = urinary incontinence; LacCer = lactosylceramide; MRC = Medical Research Council; NCV = nerve conduction velocity; SEP = somatosensory evoked potential; SNAP = sensory nerve action potential.
↓ = reduction.
[a] Optical density ratio: >3 3+; 2< 2+ <3; 1< 1+ <2; 0.3< ± <1; 0.3< –.

Figure 1 Serial neuroradiologic images for patient 1

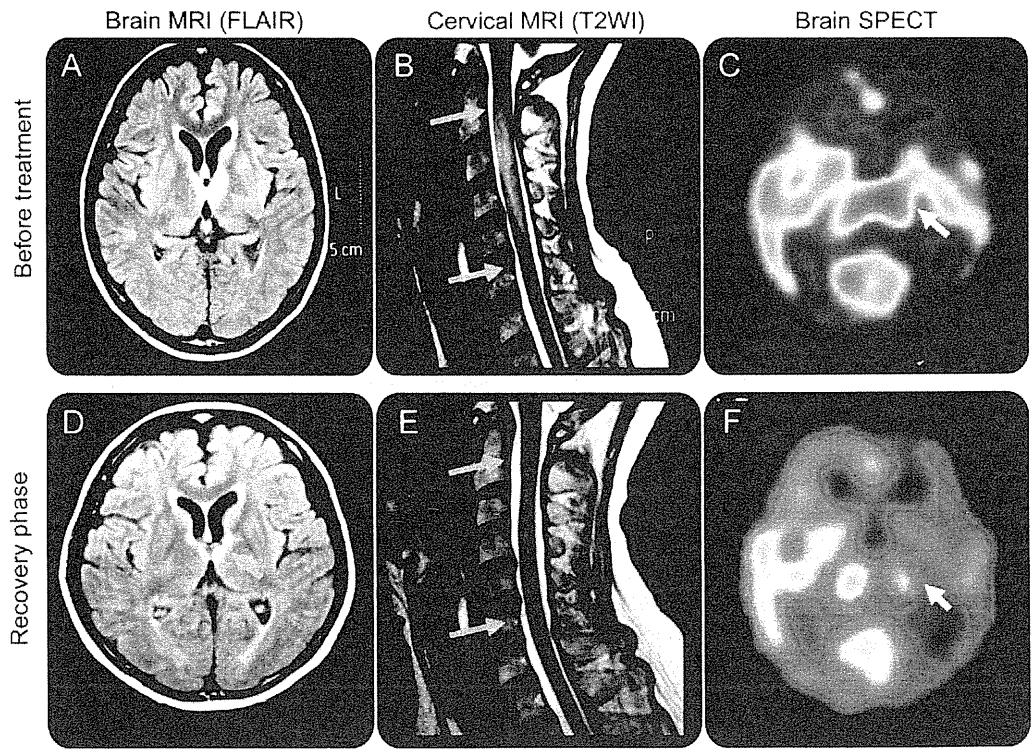

(A) Axial fluid-attenuated inversion recovery (FLAIR)-weighted brain MRI. (B) Sagittal T2-weighted (T2WI) cervical spinal cord MRI. (C) Brain SPECT obtained on day 3. (D-F) The same examinations obtained on day 52. The areas of high signal intensity on both the brain and spinal cord MRI on day 3 resolved by day 52. Arrows indicate lesions with high signal intensity on brain MRI that corresponded to high uptake areas on brain SPECT.

Figure 2 **Representative Far-Eastern blotting of neutral GSLs, and preabsorption of serum samples with a mixture of LacCer, GalCer, and GlcCer followed by Far-Eastern blot analysis**

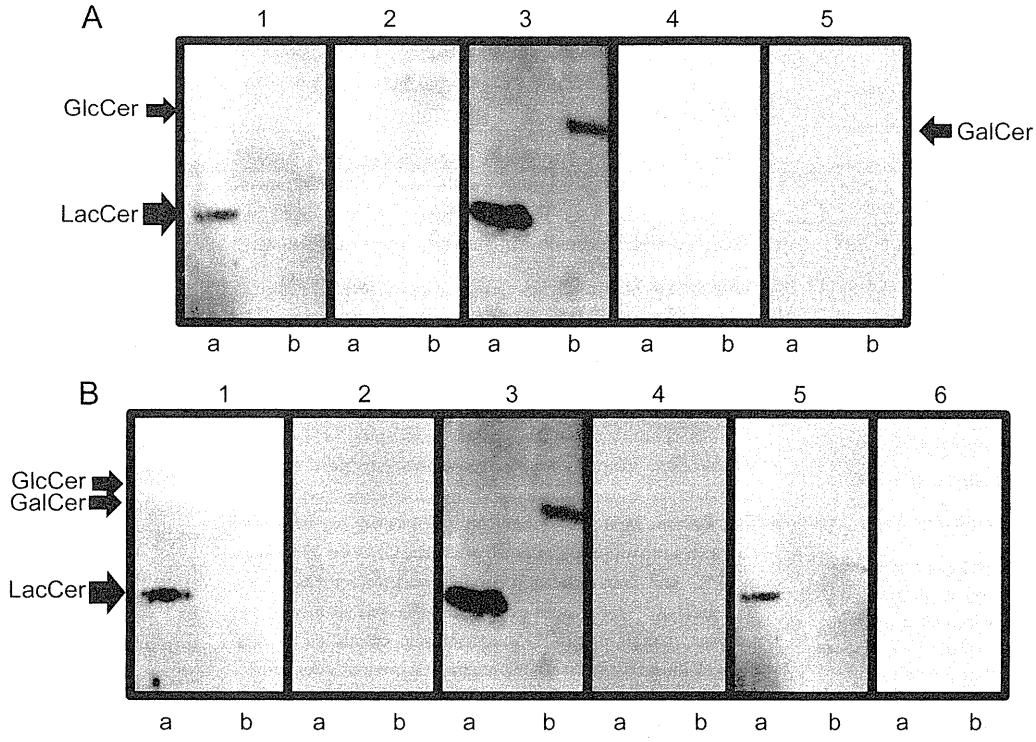

(A) Purified GlcCer, GalCer, and LacCer processed by thin-layer chromatography were electrothermally blotted onto a polyvinylidene difluoride membrane (Far-Eastern blotting). The membrane was probed with serum samples from patient 1 obtained before (1) and after (2) combined immunotherapy, serum samples from patient 2 before (3) and after (4) combined immunotherapy, and serum from a healthy volunteer (5). The position of each neutral glycolipid was determined on a thin-layer chromatography plate stained with anisaldehyde reagent.[9] We performed these experiments at least 3 times using different serum samples, with essentially identical results. Representative blots are shown. Note that serum obtained before immunotherapy from patient 1 was only positive for LacCer (immunoglobulin G fraction), whereas serum from patient 2 was positive for LacCer and to a lesser extent GalCer (immunoglobulin G fraction). In contrast, serum samples obtained from patients with EMRN after treatment and from 28 healthy volunteers showed no reactivity against these GSLs. Arrows indicate positions of LacCer, GlcCer, and GalCer. (B) Serum samples from patients with EMRN were preabsorbed with 0.1 μg each of the 3 neutral GSLs (LacCer, GalCer, and GlcCer) at 37°C for 30 minutes. These preabsorbed samples were used for further analysis. Serum from patient 4 before (1) and after (2) preabsorption with neutral GSLs, from patient 2 before (3) and after (4) preabsorption, and from patient 1 before (5) and after (6) preabsorption was used for further analysis. Serum preabsorbed with neutral GSLs was not reactive against these antigens, suggesting that antibodies against these glycolipids caused initial positive reactivity. These experiments were performed at least 3 times with essentially identical results. Representative results are shown. Arrows indicate positions of LacCer, GlcCer, and GalCer. EMRN = encephalomyeloradiculoneuropathy; GalCer = galactosylceramide; GlcCer = glucosylceramide; GSL = glycosphingolipid; LacCer = lactosylceramide.

We administered steroid pulse therapy (1,000 mg/d) for 3 days followed by high-dose IV immunoglobulin (0.4 g/kg/d) for 5 days. The patient's clinical condition and CSF, MRI, and SPECT findings improved (figure 1, D–F). She was fully recovered after 6 months.

Patient 2. A 49-year-old man was hospitalized because of a decreased level of consciousness, 1 week after the onset of flu-like symptoms. Neurologic examination revealed left facial nerve palsy, autonomic dysfunction, and tetraplegia with generalized hyperreflexia (table). Laboratory examination showed mild inflammatory reaction, but no autoantibodies. Brain gadolinium-enhanced T1-weighted images showed increased signal intensity along the meninges, and cervical MRI showed an edematous spinal cord. SPECT showed increased uptake in the right temporal and parietal lobes. Neurophysiologic and CSF examination findings were abnormal (table). After immunomodulatory treatment, the patient rapidly became alert and the radiologic abnormalities resolved.

Patient 3. The clinical findings of this 26-year-old man are shown in the table. His laboratory data were normal except for an abnormal antidiuretic hormone level. Brain MRI showed lesions with high signal intensity in the corpus callosum, and we noted increased cerebral blood flow on SPECT.

On the fourth hospital day, the patient became deeply comatose and required mechanical ventilation. After immunomodulatory treatment, his motor weakness improved and his respiratory dysfunction resolved. After 2 months, all neurophysiologic and radiologic abnormalities resolved.

Patient 4. The clinical details of this 76-year-old woman are shown in the table. The patient had abducens nerve palsy and autonomic dysfunction. Laboratory data were negative, but neurophysiologic examination findings were abnormal. We saw no lesions on brain MRI.

After IV immunoglobulin treatment, the patient's cranial nerve dysfunction resolved and her sensory and motor function gradually improved over the following month.

Sera from patients and healthy volunteers. Sera were obtained from freshly clotted blood and stored immediately in aliquots at −80°C until assayed. For comparison, we obtained serum samples from 47 age- and sex-matched patients with other neurologic disorders (8 with multisystem atrophy, 4 with neuromyelitis optica, 20 with chronic inflammatory demyelinating polyradiculoneuropathy, and 15 with multiple sclerosis) and from 28 age-matched healthy volunteers.

Standard protocol approvals, registrations, and patient consents. All study participants provided written informed consent for inclusion in this study. The Review Boards for Bioethics of Fujita Health University and Juntendo University approved this study.

Far-Eastern blot analyses using human sera. Far-Eastern blot analyses were performed using both acidic and neutral GSLs (Matreya, Pleasant Gap, PA) as described previously.[8,9] Polyvinylidene difluoride membrane was treated with human sera (×500 to ×2,000 dilution) in blocking buffer (2% nonfat milk in phosphate-buffered saline containing 1% Triton X-100). After treatment with a second antibody, positive bands were detected using enhanced chemiluminescence (PerkinElmer Inc., Boston, MA). To examine antigen identity, we incubated sera with a mixture of 0.1 μg each of neutral GSLs for 30 minutes at 37°C, and these preabsorbed sera were used for Far-Eastern blot analysis.[10] For quantification, we subjected all membranes to image analysis using NIH Image software, calculating the ratio of signal intensity to background intensity as previously described.[10]

Surface plasmon resonance analysis. See appendix e-1 on the *Neurology*® Web site at www.neurology.org.

RESULTS Clinical summary. The table shows the clinical details of the 4 patients with EMRN. All had acute or subacute motor weakness, acutely or subacutely decreased level of consciousness, brainstem dysfunction, and mild CSF pleocytosis, as well as negative antiviral antibody titers (including HIV) and real-time PCR assays for viral genomes in the CSF.

Detection of anti-neutral GSL antibodies. In all patients with EMRN, acute-phase serum samples showed clear positive bands corresponding to lactosylceramide (LacCer) (figure 2A, lane 1). In 2 patients, we noted a weak band corresponding to galactosylceramide (GalCer) (figure 2A, lane 3). In contrast, recovery-phase serum samples did not show reactivity against neutral GSLs (figure 2A, lanes 2 and 4). Patients with other neurologic disorders and 28 healthy volunteers did not have reactivity against neutral GSLs (data not shown). Anti-neutral GSL antibody titers are shown in the table.

Serum samples that were preabsorbed with a mixture of neutral GSLs did not show any positive bands, suggesting that initial positive reactivity was caused by antibodies against these GSLs (figure 2B, lanes 2, 4, and 6). Acute-phase CSF of patients with EMRN was weakly positive for GalCer and none of the sera had positive reactivity against any gangliosides (data not shown).

Surface plasmon resonance analysis. Surface plasmon resonance examination of serum samples from patients with EMRN showed antibodies against LacCer (figure e-1, patient 1) and to a lesser extent GalCer (figure e-1, patients 2 and 3). Control serum samples did not show any reactivity (figure e-1).

DISCUSSION The predominant symptoms we observed in the 4 patients with EMRN were acute motor weakness and a decreased level of consciousness. Radiologic examinations showed abnormalities of the brain and spinal cord, and electrophysiologic studies indicated dysfunction of the spinal cord, nerve roots, and peripheral nerves. Very few cases of EMRN have been reported, and most responded well to immunotherapy, similar to the patients described herein.[3,4]

GalCer is a major GSL in the cell membranes of myelin-forming cells such as oligodendrocytes and Schwann cells. Anti-GalCer antibody causes a demyelinating disorder of the PNS in rabbits.[e1] LacCer is distributed throughout the body, including the CNS, PNS, and peripheral blood cells such as neutrophils.[e2–e5] In human neutrophils, binding of anti-LacCer antibody to the LacCer domains stimulates superoxide production and phagocytosis.[e5] Although this report involves a small number of patients, our results strongly suggest that anti-neutral GSL antibodies can be used as biomarkers for EMRN.

AUTHOR CONTRIBUTIONS

Dr. Shima performed data acquisition, analysis, and manuscript drafting. Drs. Kawamura, Ishikawa, Niimi, and Ueda performed patient evaluation, data acquisition, and analysis. Drs. Masuda, Iwahara, and Iwabuchi analyzed and interpreted surface plasmon resonance analysis data. Dr. Mutoh was involved in study design, scientific supervision, and drafting and revising of the manuscript.

STUDY FUNDING

Partly supported by a grant-in-aid for the MEXT-Supported Program for the Strategic Research Foundation at Private Universities and Scientific Research (C) from the Ministry of Education, Culture, Sports, Science and Technology of Japan, and a Research Grant for Intractable Diseases from the Ministry of Health, Labor and Welfare of Japan to T.M.

DISCLOSURE

The authors report no disclosures relevant to the manuscript. Go to Neurology.org for full disclosures.

Received May 15, 2013. Accepted in final form September 26, 2013.

REFERENCES

1. Lisak RP, Zweiman B, Burns JB, et al. Immune responses to myelin antigens in multiple sclerosis. Ann NY Acad Sci 1984;436:221–230.
2. Kesselring J, Miller DH, Robb SA, et al. Acute disseminated encephalomyelitis: MRI findings and the distinction from multiple sclerosis. Brain 1990;113:291–302.
3. Blennow G, Gamstrop I, Rosenberg R. Encephalo-myeloradiculo-neuropathy. Dev Med Child Neurol 1968;10:485–490.
4. Itokazu N, Kodama Y, Kontani S, et al. A case of acute polyradiculoneuritis with multiple cranial nerve palsy and cerebral lesion: possible evidence of encephalo-myeloradiculo-neuropathy. Brain Dev 1998;30:423–429.

5. Kinoshita K, Hayashi M, Miyamoto K, Oda M, Tanabe H. Inflammatory demyelinating polyradiculitis in a patient with acute disseminated encephalomyelitis (ADEM). J Neurol Neurosurg Psychiatry 1996;60:87–90.
6. Rubin M, Karpati G, Carpenter S. Combined central and peripheral myelinopathy. Neurology 1987;37:1287–1290.
7. Mihara T, Mutoh T, Yoshikawa T, et al. Postinfectious myeloradiculoneuropathy with cranial nerve involvements associated with human herpesvirus 7 infection. Arch Neurol 2005;62:1755–1757.
8. Mihara T, Ueda A, Hirayama M, et al. Detection of new anti-neutral glycosphingolipids antibodies and their effects on Trk neurotrophin receptors. FEBS Lett 2006;580:4991–4995.
9. Mutoh T, Kawamura N, Hirabayashi Y, et al. Abnormal cross-talk between mutant presenilin 1 (I143T, G384A) and glycosphingolipid biosynthesis. FASEB J 2012;26: 3065–3074.
10. Ueda A, Shima S, Miyashita T, et al. Anti-GM1 antibodies affect the integrity of lipid rafts. Mol Cell Neurosci 2010; 45:355–362.